

# Ultrasound Spatial Compound Scanner for Improved Visualization in Vascular Imaging

S. K. JESPERSEN<sup>1</sup>, J. E. WILHJELM<sup>2</sup> & H. SILLESEN<sup>3</sup>

Center for Arteriosclerosis Detection with Ultrasound (CADUS)

E-mail: wilhjelm@it.dtu.dk. Homepage: <http://www.it.dtu.dk/~wilhjelm/cadus.html>

<sup>1</sup>B-K Medical A/S, Sandtoften 9, DK-2820 Gentofte, Denmark, <sup>2</sup>Dept. of Information Tech., Tech. Univ. of Denmark, Bldg. 344, DK-2800 Lyngby, Denmark. <sup>3</sup>Dept. of Vascular Surgery, Gentofte University Hospital, DK-2900 Hellerup, Denmark.

## ABSTRACT

A new off-line multi-angle ultrasound compound scanner has been built with the aim of improving visualization of vascular tissue. Images are recorded from 3 to 11 insonification angles over a range of 40 to 50 degrees and the individual images are combined (averaged) into a single image (spatial compounding). Compared to conventional B-mode imaging, this multi-angle compound imaging (MACI) method features less angle-dependent images, since more scan lines are nearly perpendicular to the tissue interfaces. Further, the spatial compounding strongly diminishes the speckle pattern. These improvements are illustrated with *in vitro* images of porcine aorta and human atherosclerotic plaque.

## 1. Introduction

The presence of atherosclerotic lesions (plaque) in the carotid arteries increases the risk of stroke, but surgical removal of the plaque has proven beneficial in reducing the risk of stroke.<sup>[2]</sup> However, ultrasonic assessment of size, shape and type of the carotid atherosclerotic lesions is often seriously limited by poor visualization of the plaque. There are several reasons for this: *i*) Some plaque materials, such as certain lipids, are echopoor in nature<sup>[4]</sup> and will always be difficult to visualize. *ii*) Other non-isotropic materials, such as fibrous tissues, produce echo signals with a strong angle-dependence<sup>[4]</sup> resulting in fluctuations in echogenicity when the transducer is moved and/or rotated. *iii*) Because the pathological thickening of the carotid wall is seldom larger than 4 mm, the region of interest on the ultrasound image is only approximately 20 wavelengths thick (assuming a transducer frequency of 7.5 MHz and a sound speed of 1540 m/s). Due to the speckle noise in this small ultrasound image region, residual lumen, plaque outline and plaque type can often be difficult to determine.

A possible solution to some of these problems is to use spatial compound imaging which can reduce the angle-dependence and the speckle noise<sup>[6,7]</sup>. Therefore, a digital off-line ultrasound scanner for multi-angle compound imaging (MACI) was built with the purpose of improving visualization of vascular tissue. This paper

describes the instrument and the *in vitro* results obtained when scanning porcine aorta and human atherosclerotic plaque.

## 2. Principle of Operation

The MACI system utilizes a conventional low-pitch linear array transducer. The active aperture is selected as a subset of the elements and this aperture is then operated in a phased array mode, to create a beam with a given angle,  $\theta_i$ . The aperture is then moved along the entire array to record an entire image at that angle. This operation is repeated for all desired beam angles,  $\theta_i$ , where  $i = 1, 2, \dots, N_\theta$ . Figure 1 illustrates the scanlines used in this procedure for  $N_\theta = 3$ . It is seen that the fully compounded region, theoretically, is a triangle. From the geometry, the depth of this region can be found to:

$$z_{max}(D, \theta_{max}, \theta_{min}) = \frac{D}{\tan(\theta_{max}) - \tan(\theta_{min})} \quad (1)$$

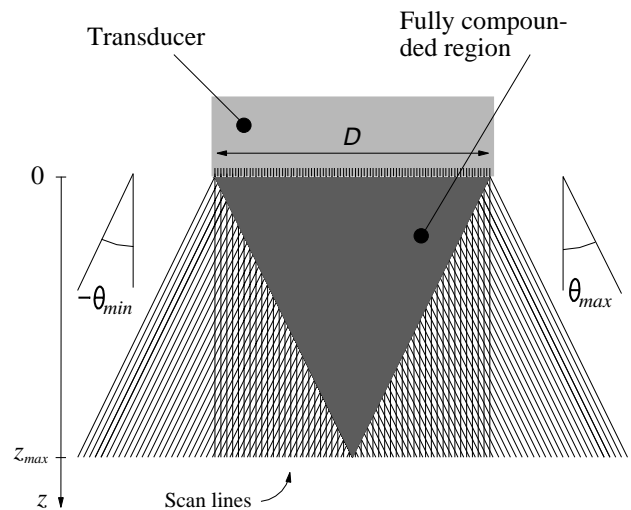


**Figure 1** Illustration of scan lines for three single-angle images used in creating the multi-angle compound image.

where  $D$  is the total array length and  $\theta_{max}$  and  $\theta_{min}$  are the most positive and the most negative beam angles, respectively. As an example, consider  $D = 40$  mm and  $\theta_{max} = -\theta_{min} = 20^\circ$ , which gives  $z_{max} = 55$  mm.

### 3. System Hardware

The system hardware shown in Figure 2 consist of three major components: *i*) A 192-element linear transducer array with center frequency 7.5 MHz, pitch 208  $\mu$ m. The array length is  $D = 40$  mm. *ii*) A control workstation containing a PCI-based 12 bit AD-card and a timing controller (Real-time scan controller, RTSC) for the ultrasound system. *iii*) A 19" rack containing the transmit and receive system hardware, power supply and transducer connector.

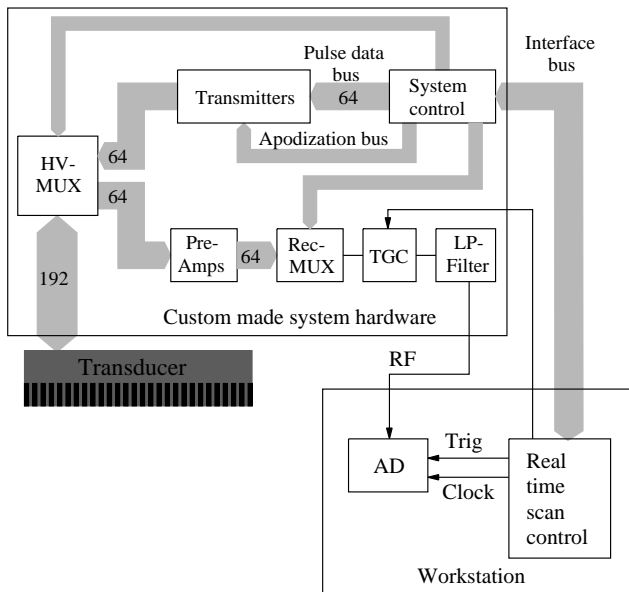


**Figure 2** Block diagram of system components.

The real-time transmit system contains 64 parallel transmitters with fully programmable transmit delays (0 - 34  $\mu$ s) and apodization control (-25 - 0 dB). The delay resolution of the transmit system is 16.7 ns. The receiver system consist of 64 parallel pre-amplifiers and a multiplexer which selects one of the receive channels (thus one single-element signal is recorded at a time). This one signal subsequently passes a time-gain control (TGC) amplifier and an anti-aliasing lowpass filter before it is digitized in the 12 bit AD-converter located in the control workstation. The signals can be digitized with a sampling frequency up to 60 MHz.

All clock signals (including ADC clock), timing signals, TGC voltage, etc., are generated by the RTSC board mounted in the control workstation. This approach yielded very low jitter between recorded single element signals, which is crucial when sampling the single element

signals one at a time and beamforming off-line. Typical recording time for a single image (192 scanlines each of 64 single element signals) is 2 to 3 minutes.

### 4. Signal Processing in Software

The system software consists of three main parts: *i*) Creation of setup data for the system, *ii*) Control of the hardware and the recording of the single element signals and *iii*) processing of the received signals.

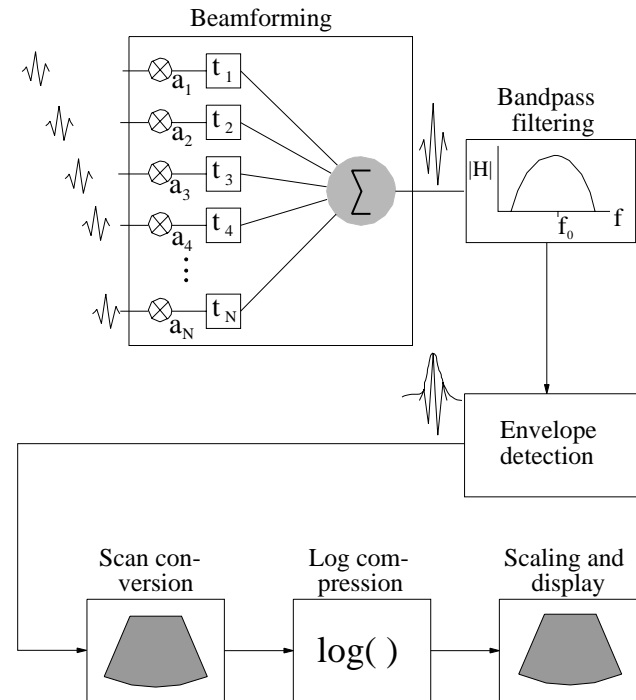


**Figure 3** Block diagram of signal processing made in software.

The elements of the digital signal processing performed on the received signals are shown in Figure 3 and consist of dynamic beamforming, bandpass filtering, envelope detection, scan conversion, logarithmization, scaling and display. The compound image is finally generated by averaging the single-angle images, however, it is only in the fully compounded region that all single-angle images contribute to this averaging.

### 5. System Characterization

The point spread function was analyzed with a custom made point scatterer phantom consisting of a single  $\sim 100$   $\mu$ m diameter glass sphere molded into the center of an agar block. The glass sphere was located  $\sim 35$  mm from the transducer. Images were recorded from 11 different angles in steps of  $5^\circ$ . The -6 dB width of the point spread function measured from the  $0^\circ$  image was 0.7 mm and 0.21 mm, in the lateral and axial directions, respectively. The same measures for the compound image were 0.77

mm and 0.27 mm, respectively. Thus, the spatial compounding increase the point spread function by no more than ~30 %.

Speckle reduction was investigated experimentally using a custom made phantom<sup>[1]</sup> consisting of a speckle generating substance (coarse grain silicon carbide) mixed with an attenuation generating substance (fine grain silicone carbide) and molded into agar. The speed of sound was 1540 m/s and the attenuation was 0.58 dB/MHz/cm. A region of size 10.7 x 3.6 mm (150 x 50 pixels) located at a depth of 25 mm was scanned with both conventional imaging and compound imaging. A numerical analysis of this region showed that in comparison to conventional imaging, the signal-to-noise ratio was increased by a factor of 2.4 and 2.6 when using 6 angles separated 10° and 11 angles separated 5°, respectively. These results are in excellent agreement with theory<sup>[5]</sup>.

## 6. Results

**Thoracic porcine aorta:** Conventional B-mode images of vessel cross-sections are generally quite angle-dependent. To investigate the benefit of spatial compounding, cross-sectional images of formalin fixed thoracic porcine aortas<sup>[8]</sup> were recorded using conventional imaging (0° image) and MACI (averaged image of -25°, -15°, -5°, 5°, 15°, 25° images). Typical results are provided in Figure 4, which shows a 200x200 pixel (21x21 mm) region centered at a depth of 25 mm. It is seen, that the outlines of the artery is better visualized when using MACI and that the speckle pattern is significantly reduced in the MACI image compared to the conventional image.

Note the appearance of a bright spot in the ten-o'clock direction in both images in Figure 4 and a bright spot in the nine-o'clock direction in the conventional image (Fig-

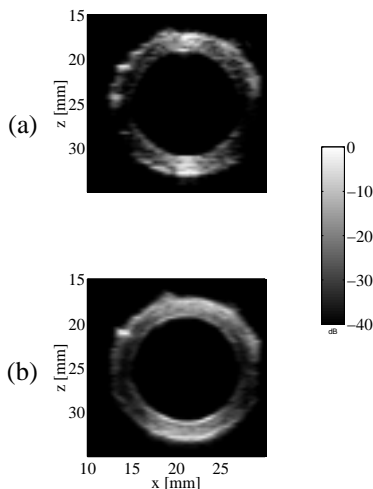


**Figure 4** Conventional (a) and compound (b) images of formalin fixed thoracic porcine aorta. See text for details.

ure 4a). The first spot is believed to be a true variation in the acoustical properties of the specimen, as it could be observed in all single-angle images (including the 0° image). On the other hand, the spot in the nine-o'clock direction did not appear in any of the single-angle images used to form the compound image. Thus, it is likely that this spot was the result of random variation in the speckle pattern.

**Carotid Atherosclerotic Plaque:** In assessment of atherosclerosis, the plaque and its outline can be very difficult to visualize well. In this case, formalin fixed carotid plaques (removed by endarterectomy) were scanned in 3D cross-sectionally and longitudinally with conventional imaging (0° image) and MACI (averaged image of -21°, -14°, -7°, 0°, 7°, 14° and 21° images). A total of 112 image sets were recorded, with a spacing of 0.5 mm between two image sets. The plaques were fixed to a special frame by means of four sutures and submerged in pure demineralized water at ~20°.

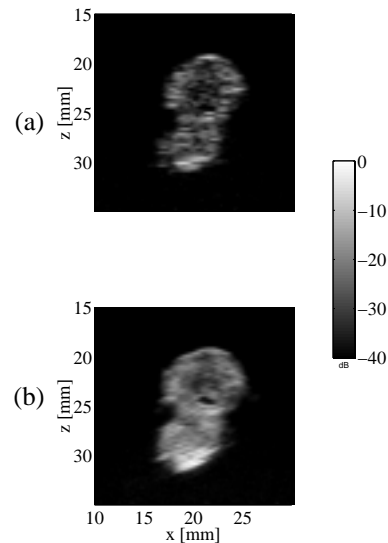


**Figure 5** (a) conventional and (b) compound cross-sectional images of atherosclerotic plaque.

Typical conventional and MACI cross-sectional images are shown in Figure 5. The size of the image regions shown here and the corresponding depth can be seen from the axis, in the same manner as in Figure 4. The images shows plaque from the internal carotid artery close to the transducer and plaque from the external carotid artery beneath it. The MACI image shows a significantly improved visualization due to the better definition of the outline and the reduced speckle. Likewise, the residual lumen is much more clearly delineated in the MACI images.

Figure 6 shows the individual single-angles images used to produce Figure 5b. Notice the rather poor definition of the outline (and the lumen) in the single-

angle images, compared to the corresponding compound image in Figure 5b.

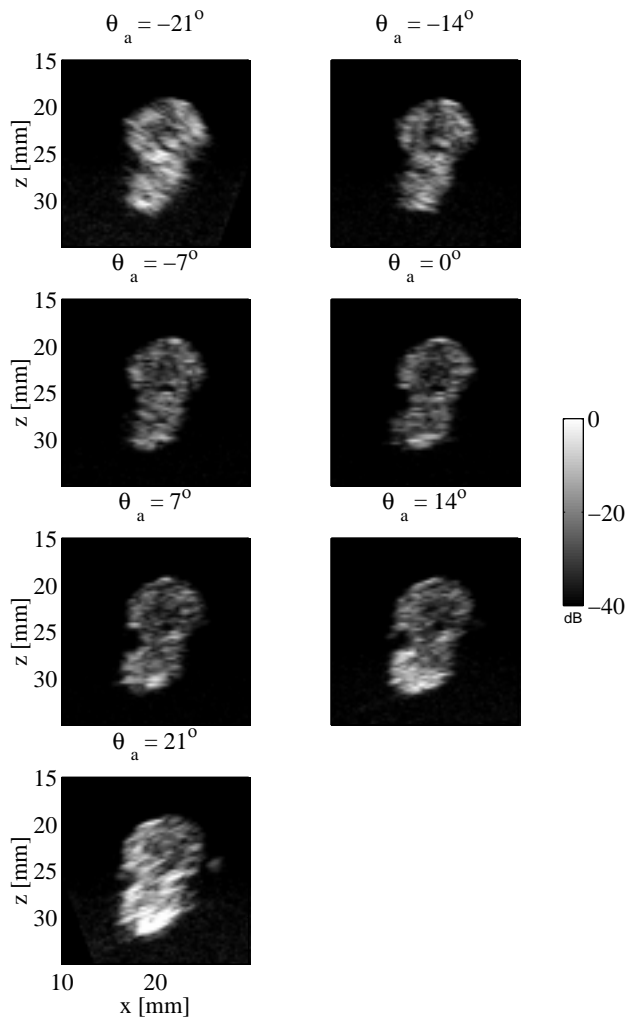


**Figure 6** The seven single-angle images used to create the compound image in Figure 5a.

## 7. Discussion

The results in Figures 4 - 5 show improved visualization of boundaries, partly due to the fact that more scanlines are nearly perpendicular to the reflecting surfaces, partly due to the reduced speckle noise. Despite the encouraging results arrived at in this investigation, it should be pointed out that a number of factors may influence the achievable image quality. Two of them are based on the fact that single images are recorded and then added.<sup>[3]</sup>

- a) Spatial variation in the speed of sound might also cause blurring, due to misalignment between the individual single-angle images.

- b) Tissue movement might cause some image blurring: because the individual single-angle images are recorded consecutively, these might not align completely when added to form the compound image.

## 8. Conclusions

A new imaging modality, Multi-Angle Compound Imaging, has been described and *in vitro* results showing reduced speckle noise and reduced angle-dependence have been presented. The results based on porcine aorta and human atherosclerotic plaque reveal a better definition of outlines and more a uniform representation of tissue parameters, compared to conventional B-mode imaging. Therefore, MACI is believed to have potential for improving diagnosis of atherosclerotic disease.

## Acknowledgements

CADUS is supported by the Danish Technical and Medical Research Councils. The authors gratefully acknowledge the help by MD M.-L. Moes Grønholdt for providing the specimens and the help by instrument maker K. Martinsen for making the fixtures for the transducer and the biological specimens.

## References

- [1] Danish Phantom Design, Jyllinge, Denmark. [www.fantom.suite.dk](http://www.fantom.suite.dk).
- [2] European Carotid Surgery Trialist' Collaborative Group (ECST). Randomized trial of endarterectomy for recently symptomatic carotid stenosis: final results of the MRC European Carotid Surgery Trial (ECST). *The Lancet*, Vol. 351, pp. 1379-1387, 1998.
- [3] Jespersen SK, Wilhjelm JE, Sillesen H: Multi-angle compound imaging. Accepted for publication in *Ultrasonic Imaging*, 1998.
- [4] Picano E, Landini L, Distanti A, Salvadori M, Lattanzi F, Masini M, L'Abbate A: Angle dependence of ultrasonic backscatter in arterial tissues: a study in vitro. *Circulation*, Vol. 72, No. 3, pp. 572-576, 1985.
- [5] Shankar PM, Newhouse VL: Speckle Reduction with Improved Resolution in Ultrasound Images. *IEEE Transactions on Sonics and Ultrasonics*, Vol. 32, No. 4, pp. 537-543. 1985.
- [6] Shattuck DP, Ramm OTv: Compound Scanning with a Phased Array. *Ultrasonic Imaging*, Vol. 4, pp. 93-107. 1982.
- [7] Trahey GE, Smith SW, Ramm OTv: Speckle Pattern Correlation with Lateral Aperture Translation: Experimental Results and Implications for Spatial Compounding. *IEEE Transactions on UFFC*, Vol. 33, No. 3, pp. 257-264. 1986
- [8] Wilhjelm JE, Vogt K, Jespersen SK, Sillesen HH: Influence of Tissue Preservation Methods on Arterial Geometry and Echogenicity. *Ultrasound in Med. & Biol.*, Vol. 23, No. 7, pp. 1071-1082. 1997.